



Effect of stabilizers and nitrogen content on thermal properties of nitrocellulose granules

Katarzyna Cieślak¹ · Katarzyna Gańczyk-Specjalska² · Katarzyna Drożdżewska-Szymańska³ · Michał Uszyński¹

Received: 29 May 2019 / Accepted: 9 January 2020 / Published online: 20 January 2020
© The Author(s) 2020

Abstract

The granules containing nitrogen of various content (12.2–13.3%) and stabilizers (centralite I, centralite II, akardite II, triphenylamine) were obtained in laboratory scale, and the study of their physicochemical and thermal properties was conducted. It has been observed that the helium density of granules depends on the degree of gelling of nitrocellulose by the stabilizer as well as the lack of effect of the stabilizer type on the heat of combustion value. In turn, the heat of combustion depends on the content of nitrogen in nitrocellulose. Granules of 13.3% N nitrocellulose were characterized by a more rapidly developing thermal decomposition than the granules containing 12.2 and 12.9% N nitrocellulose. The maximum temperature of decomposition shifts toward higher temperatures (from 207.6 to 209.8 °C) with decreasing nitrogen content in nitrocellulose for granules containing triphenylamine as a stabilizer. All values of heat generation rate obtained for granules with triphenylamine were lower than the respective rates for granules with centralite I. Thermal properties and chemical stability of granules containing triphenylamine have better properties, when compared to other examined stabilizers. On the basis of differential scanning calorimetry and thermogravimetry, kinetic parameters were calculated by means of Ozawa–Flynn–Wall analysis. The effect of stabilizers and nitrogen content on kinetic parameters was determined. The kinetic model of thermal decomposition of granules was adjusted—the best fit was *n*th-order reaction with autocatalysis. The activation energy of thermal decomposition process according to the adopted chemical reaction model increases from 190 to 239 kJ mol⁻¹ with increasing nitrogen content in the granulate.

Keywords Nitrocellulose · Stabilizer · Nitrogen content · Thermal properties · Kinetic parameters

Introduction

Cellulose belongs to polysaccharides and can be found in natural environment (e.g., cotton, flax and spruce). The product of esterification of cellulose and nitric acid is an energetic polymer—nitrocellulose (NC). Each monomer in cellulose consists of three hydroxyl groups which may react with a nitrating mixture. Through the selection of composition of nitrating mixture, temperature and time, NC of various nitrogen contents can be obtained. Such parameters of this polymer as solubility, hygroscopicity, viscosity, stability and utility features depend on the nitrogen content in the nitrocellulose structure [1, 2]. Nitrocellulose is characterized by low stability. During extended storage of the polymer, nitrogen oxide compounds can be emitted due to a low value of bond energy (155 kJ mol⁻¹) of ester functional group –CH₂O–NO₂ [3, 4]. These nitrogen oxide compounds lead to destabilization of NC. In order to prevent this process from taking place, stabilizers for nitrocellulose products are

Electronic supplementary material The online version of this article (<https://doi.org/10.1007/s10973-020-09304-8>) contains supplementary material, which is available to authorized users.

✉ Katarzyna Gańczyk-Specjalska
specjalska@ipo.waw.pl

¹ Division of High Energetic Materials, Faculty of Chemistry, Warsaw University of Technology, Noakowskiego 3, 00-664 Warsaw, Poland

² Department of High Energetic Materials, Lukasiewicz Research Network – Institute of Industrial Organic Chemistry, Annopol 6, 03-236 Warsaw, Poland

³ Chemical Safety and Static Electricity Department, Lukasiewicz Research Network – Institute of Industrial Organic Chemistry, Annopol 6, 03-236 Warsaw, Poland

introduced. These additives do not hinder decomposition process entirely and, however, may contribute to the reduction of autocatalytic effect of decomposition. Most stabilizers act based on the principle of chemical interactions, which include binding the products of decomposition [5, 6]. Derivatives of urea or aniline such as centralite, diphenylamine, akardite and 2-nitrodiphenylamine constitute the most commonly used stabilizers [6, 7]. Other stabilizers are investigated, as derivatives of urea and aniline produce carcinogenic nitrosamines by reaction with nitrogen oxides. Furthermore, diphenylamine (DPA) has toxic properties [3]. For this reason, new compounds are proposed as stabilizers for nitrocellulose, such as triphenylamine (TPA) [4], deprived of toxic properties. The reaction of this stabilizer with nitric oxides leads to the formation of nitro derivatives.

During aging process, primary or secondary amines (e.g., DPA) form *N*-nitroso derivatives which have toxic properties. Stabilizing properties of TPA are comparable to the properties of DPA, which has been confirmed by the study of stabilizer consumption under the influence of nitrogen oxides. A similar degree of depletion was obtained for investigated stabilizers [8]. During aging of TPA-containing powders, stabilizer is consumed faster than in the case of powders containing centralite I, akardite II or 2-nitrodiphenylamine [9]. TPA is a more effective stabilizer for single-base than for two-base powders [4]. New, non-toxic, environmentally friendly compounds (such as tocopherol or ionone derivatives) have also been offered as stabilizers [10–12]. Derivatives of these substances have been determined as being non-toxic and having stabilizing properties of nitrocellulose propellants [13].

One of the major applications of nitrocellulose includes the production of propellants. Relevant physicochemical properties of nitrocellulose (such as solubility in different solvents, viscosity) resulted in manufacturing process involving various shapes of propellant grains, e.g., flakes, cylinders or spherical shapes. Spherical grains of nitrocellulose are obtained by water [14, 15] or lacquer method [16, 17]. The granulation process is obtained by a damage of fiber nitrocellulose structure caused by processing of solvent. In water method, NC is suspended in water and subsequently is added to solvent. In granulation process, such solvents as esters or ketones, e.g., ethyl acetate, butyl acetate, isopropyl acetate, isobutyl methyl ketone, methyl phenyl ketone are used [14, 16–20]. Nitrocellulose stabilizers can be added with a process solvent. The next step of granulate formation includes the addition of protective colloid in order to reinforce formed NC granules. Gelatin, dextrin, potato or corn starch, animal glue, acacia gum [20–22] are used as protective colloids. Water (trapped inside NC granules) is removed by the solution of inorganic salt (e.g., sodium sulfate, potassium nitrate, barium nitrate). At the end of the process, the solvent is distilled off. Spherical nitrocellulose powders can be used for

technological process of gun propellants [23] or homogeneous rocket propellants [24].

The knowledge of kinetic parameters of decomposition process of high energetic materials is quite important as regards the safety of use or storage conditions. A thermal explosion may take place during uncontrolled decomposition, which can be observed from low degrees of conversion [25–27]. Kinetic parameters of thermal decomposition for pure nitrocellulose, nitrocellulose mixtures with stabilizers, or smokeless powder have been widely reported in the literature [4, 28–37]. Nitrocellulose demonstrates differences in a determined activation energy, depending on the size of fibers. For nanofibers, a value of 105 kJ mol⁻¹ was determined, whereas 157 kJ mol⁻¹ in case of microfibers (Ozawa method) [37]. For nitrocellulose of 12.76% nitrogen content, activation energy was determined with the measurements taken by means of isothermal decomposition dynamics research instrument [38]. The activation energy determined by Arrhenius equation amounted to 145.6 kJ mol⁻¹, whereas for model fitting method – 144.7 kJ mol⁻¹. The activation energy of decomposition for homogenous thin film (content of nitrocellulose of 12.6% N and 3%_{mass} stabilizer) was calculated by Ozawa–Flynn–Wall method based on differential scanning calorimetry (DSC). The results of measurements for pure nitrocellulose were as follows: 140 kJ mol⁻¹, NC+DPA 190 kJ mol⁻¹, NC+N-(2-methoxyethyl)-*p*-nitroaniline (MENA) 186 kJ mol⁻¹, NC+eutectic (DPA+MENA) 200 kJ mol⁻¹ [31]. The activation energy of decomposition for single-base propellants obtained by solvent or non-solvent method amounted to the following: 148 kJ mol⁻¹, (3%_{mass} centralite I, DSC test, Ozawa method) [32], 114–118 kJ mol⁻¹ (1%_{mass} DPA, akardite I or akardite II, microcalorimetry test and isoconversional evaluation), 129–133 kJ mol⁻¹ (1%_{mass} TPA, microcalorimetry test and isoconversional evaluation) [4]. The differences in activation energy resulted from measurements conditions, method used, nitrocellulose, type and content of stabilizer and type of examined material [39, 40].

The aim of the study was to extend the state of knowledge on the effect of stabilizers and nitrogen content on thermal properties of nitrocellulose. The following stabilizers were chosen: centralite I, centralite II, akardite II and triphenylamine. Furthermore, the effect of nitrogen content on the properties of obtained nitrocellulose granules was investigated. The following parameters were studied for the resultant granules: helium density, volume fraction of closed pores, heat of combustion, thermal properties and kinetic parameters of thermal decomposition.

Table 1 The properties of nitrocellulose used

Symbols of used NC	12.2% N	12.9% N	13.3% N
Nitrogen content %	12.18 ± 0.18	12.94 ± 0.04	13.28 ± 0.04
Viscosity/°E	2.1–2.6	4–8	4–8
Fineness/mL	Max 95	90–105	90–105
Solubility in ethanol	Max 12%	Max 5%	Max 4%
Volume of emitted nitrogen oxides (Bergmann-Junk method)	Max 2.5 mL	Max 2.5 mL	Max 2.5 mL

Table 2 Symbols of granulation products, types of nitrocellulose and stabilizers

Symbol of granulation product	NC type	Stabilizer type
G(CI)1	12.2% N	Centralite I
G(CI)2	12.9% N	
G(CI)3	13.3% N	
G(TPA)1	12.2% N	Triphenylamine
G(TPA)2	12.9% N	
G(TPA)3	13.3% N	
G(CII)3	13.3% N	Centralite II
G(AkaII)3	13.3% N	Akardite II

Materials and methods

Materials

The products used in the granulation process included nitrocellulose (NC) with various nitrogen content: 12.2%, 12.9% and 13.3% (the properties of used NC are summarized in Table 1); stabilizers: centralite I (min. 93% assay), centralite II (min. 97% assay), akardite II (min. 99% assay) purchased from MESKO S.A. Pionki Branch (Poland); triphenylamine (min. 99% assay) purchased from Sigma-Aldrich®; ethyl acetate (min 99% assay), potato starch and sodium sulfate anhydrous purchased from Chempur®.

Nitrocellulose granulation process

The nitrocellulose granules were prepared in laboratory scale. Eight granulation processes were performed for each type of nitrocellulose and stabilizers. Symbols of each product are presented in Table 2.

Nitrocellulose (18.0 g calculated on dried NC) was suspended in 305 mL of distilled water in a reactor with four-blade propeller stirrer. The mixture was heated to 50 °C, and then 116 mL of ethyl acetate (EtAc) with 0.27 g of

stabilizer was dosed to nitrocellulose suspension with dropping funnel. After 30 min, 0.27 g of potato starch in 20 mL of distilled water was added to mixture; after another 30 min, sodium sulfate (13.2 g) in 100 mL of distilled water was added to reactor. A final step involved the distillation of EtAc by heating up gradually to max 95 °C. Obtained granules were sieved in a stream of water on sieves of the following dimensions: 0.385 and 0.75 mm. Each portion of NC grains was dried to constant mass at 60 °C.

Methods

The measurements of density were performed by using helium pycnometer Micrometrics AccuPyc 1330 at a temperature of 23.1 ± 0.5 °C (volume of samples 0.6 cm³). Ten measurements were taken for individual samples, which served to calculate the mean and standard deviation.

Heat of combustion analysis was performed using adiabatic bomb calorimeter IKA C2000 Basic. Samples (2.00 g) were placed in the bomb under reduced pressure. The calorimeter was calibrated by burning a standard propellant. Two measurements were taken for individual samples, which served to calculate the mean and standard deviation.

The analysis of thermochemical properties was carried out by NETZSCH STA 449F1 calorimeter (simultaneous analysis of differential scanning and thermogravimetric calorimetry—DSC-TG). Samples of approx. 0.8 mg were placed in aluminum pans (Concavus® type) and measured in the temperature range of 30–300 °C and at five different heating rates in the range of $\beta = 1–10$ °C min⁻¹. The measurements were taken under nitrogen atmosphere with a gas flow of 70 mL min⁻¹. The measurements were repeated twice for $\beta = 5$ °C min⁻¹ to compare thermal decomposition of each granules and three times for $\beta = 1$ and 10 °C min⁻¹ to calculate kinetic parameters of thermal decomposition. The collected experimental data for kinetic computations were calculated in accordance with recommendations of International Confederation for Thermal Analysis and Calorimetry (ICTAC) [41]. DSC-TG diagrams were interpreted by NETZSCH Proteus—Thermal Analysis version 6.1.0 software, and kinetic parameters were calculated by Thermokinetics 3.1 software (NETZSCH).

Heat flow calorimetry (HFC) was conducted with use of TAM III calorimeter (TA Instruments). Samples were placed in capped ampoules (2.0 g). Measurements were determined at 90 °C (the highest temperature recommended by standard STANAG 4582 procedure [42]), and calorimetric signal analysis started after 45 min according to manufacturer recommendation. A total duration of measurement amounted to min. 3.9 day.

Theory and calculation

The calculation of kinetic parameters revealed that many parallel and consequent reactions take place during thermal decomposition of nitrocellulose granules. For this reason, the kinetic description is used in quite generic terms. It has been assumed that nitrocellulose decomposition is consistent with the primary model [2, 37], and the products of decomposition have decomposition-catalyzing properties.

The authors of the publication [43] proposed an equation describing the dependence of heat cumulative ($Q_{\text{cumulative}}$) over time for HFC measurements. Using the same assumptions, a heat generation rate (k_Q) was determined according to the equation:

$$Q_{\text{cumulative}} = t \cdot k_Q + c \quad (1)$$

where t is time, c integration constant.

Calculated kinetic parameters were based on all reactions occurring simultaneously, therefore the term apparent activation energy (${}_aE_a$) was introduced to describe the kinetic parameters. The apparent activation energy and logarithm of pre-exponential factor were calculated using Ozawa–Flynn–Wall isoconversional method according to the ICTAC recommendation [39, 44–46]. This method is the integral method, which leads to $-{}_aE_a/R$ determined from the slope of the line determined by plotting $\ln\beta$ against $1/T$ at any certain conversion rate. The applied equation is as follows:

$$\ln \beta = C - 1.052 \cdot ({}_aE_a/RT) \quad (2)$$

where β is heating rate, T temperature, R gas constant and C constant.

Results and discussion

The research was divided into two parts: the effect of stabilizers as well as nitrogen content in nitrocellulose on the properties of obtained nitrocellulose granules. Helium density (ρ_{He}), volume fraction of closed pores (P_c), heat

of combustion (Q_c) and thermal and kinetic parameters of thermal decomposition for the obtained products were determined. Fraction of 0.385–0.750 mm of granules was used for all measurements with the exception of DSC/TG examination, where fraction below 0.385 mm was applied.

The effect of stabilizer on the properties of nitrocellulose granules

The results of examination of helium density, volume fraction of closed pores and heat of combustion of granules are presented in Table 3. Helium density for CI- and TPA-containing granules is similar and lower than in case of other two granules (containing AkaII and CII). Helium density is also associated with the volume fraction of closed pores—this accounts for the difference in the maximum density of nitrocellulose and the one measured for the granulate in relation to the maximum density of nitrocellulose. The maximum density of nitrocellulose is 1.67 g cm^{-3} [47]. The volume fraction of pores closed in granules G(CI)3 and G(TPA)3 amounts to approx. 9.5% and is higher by approx. 2.0% in relation to other two granules (containing AkaII and CII). The differences in helium densities (and therefore in the volume fraction of closed pores) may be related to varying level of gelation of nitrocellulose during granulation. A more compact structure of nitrocellulose (smaller number of closed pores) can be obtained once the nitrocellulose has been gelled more extensively. The lowest value of the heat of combustion was characteristic to G(CII)3, while the highest value was observed for granules G(CI)3 and G(AkaII)3—the difference between these granules amounted to 132 J g^{-1} . The introduced amount of stabilizer should not significantly affect the heat of combustion value; therefore, theoretical thermodynamic calculations were conducted by means of “The ICT-Thermodynamic-Code” (ICT-Code) program. The pressure of 0.1 bar was adopted for the sake of calculation. Theoretical heat of combustion rates amounts to the following: 4095 J g^{-1} for G(CI)3, 4074 J g^{-1} for G(TPA)3, 4100 J g^{-1} for G(CII)3, and G(AkaII)3. The maximum difference of 26 J g^{-1} confirms that the change of stabilizer does not significantly affect this parameter.

Table 3 The properties of examined granules containing various stabilizers (CI, CII, TPA, AkaII)

Samples	G(CI)3	G(TPA)3	G(AkaII)3	G(CII)3
$\rho_{\text{He}}/\text{g cm}^{-3}$	1.507 ± 0.004	1.516 ± 0.007	1.550 ± 0.007	1.542 ± 0.003
$P_c/\%$	9.75 ± 0.26	9.20 ± 0.43	7.19 ± 0.44	7.66 ± 0.17
$Q_c/\text{J g}^{-1}$	3630 ± 38	3619 ± 33	3631 ± 5	3499 ± 23
$T_{\text{onset}}/^\circ\text{C}$	193.9	193.0	193.4	193.3
$T_{\text{max}}/^\circ\text{C}$	202.4	202.7	202.6	202.2
$\Delta H_d/\text{J g}^{-1}$	2258	2234	2110	2045
$P_f/\mu\text{W g}^{-1}$	53.1	30.3	35.7	43.6
$k_Q/\text{J g}^{-1} \text{ days}^{-1}$	3.93 ± 0.01	2.18 ± 0.01	3.37 ± 0.01	3.57 ± 0.01

DSC curves of G(CI)3, G(CII)3, G(AkaII)3 and G(TPA)3 granules are presented in Fig. 1. One exothermic transition (thermal decomposition) took place in the temperature range of 180–240 °C for these samples. The shapes of obtained peaks are similar to each other for all granulates with different stabilizers.

The values of thermal properties, i.e., onset temperature (T_{onset}), maximum temperature (T_{max}) and enthalpy of decomposition (ΔH_d), are shown in Table 3. It was observed that the type of stabilizer has not an impact on the maximum temperature of exothermic process—the difference between the minimum and maximum value is 0.8 °C. The enthalpy values of decomposition for G(CI)3 are the highest from all studied granules (average value is 2246 J g⁻¹). The enthalpy

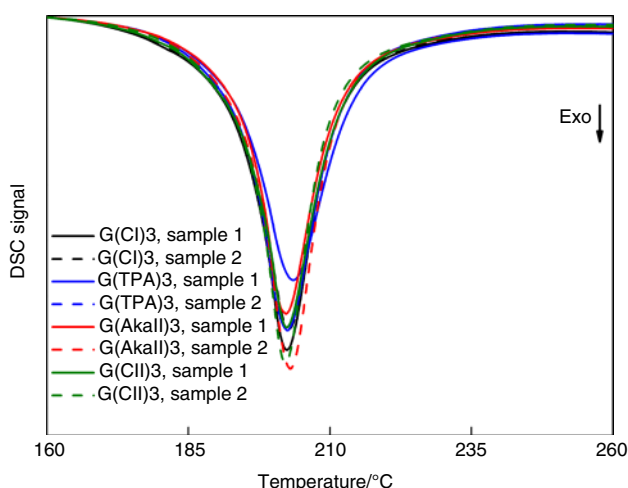


Fig. 1 DSC curves of nitrocellulose (13.3% N) containing granules and various stabilizers (centralite I, centralite II, triphenylamine, akardite II)

values of decomposition are lower about 100 J g⁻¹ for the rest obtained granules containing TPA, AkaII and CII as a stabilizer.

The relationship between heat flow and time (HFC curves) as well as cumulative heat ($Q_{\text{cumulative}}$) versus time for granules containing different stabilizers is presented in Fig. 2. A gray, continuous line demonstrates a linear regression according to Eq. (1) in Fig. 2b. Granules containing CI, TPA and CII are characterized by a similar course of curves with a visible local minimum (for 1.77 days for G(CI)3, 2.10 days for G(CII)3 and 2.47 days for G(TPA)3). The heat flow signal increases in the initial stage for G(AkaII)3 and then decreases until the end of the measurement. The shape of these curves probably is related to stabilizer depletion and formation new derivatives. Tomaszewski et al. [43] observed such behavior for single-base propellants containing diphenylamine. The heat flow signal in time $t_m = 3.43$ day (P_l) for all granules is contained below 60 $\mu\text{W g}^{-1}$, which is the value more than 6 times lower than the maximum allowable heat flow in STANAG 4582 (350 $\mu\text{W g}^{-1}$). All examined granules conform to the requirements of STANAG 4582, which means that they remain stable in storage conditions in 25 °C for 10 years. P_l and heat generation rate (k_Q) values are summarized in Table 3. The heat generation rate decreases for granules in the following order: G(CI)3 > G(CII)3 > G(AkaII)3 > G(TPA)3. Katoh et al. [5] obtained a similar dependence. Triphenylamine containing granule has the lowest heat generation constant and the lowest heat flow after 4 days of measurements, as compared to other granules containing conventional stabilizers.

The addition of triphenylamine into nitrocellulose granules does not entail significant changes in density, volume fraction of closed pores and the heat of combustion when compared to the granules containing conventional

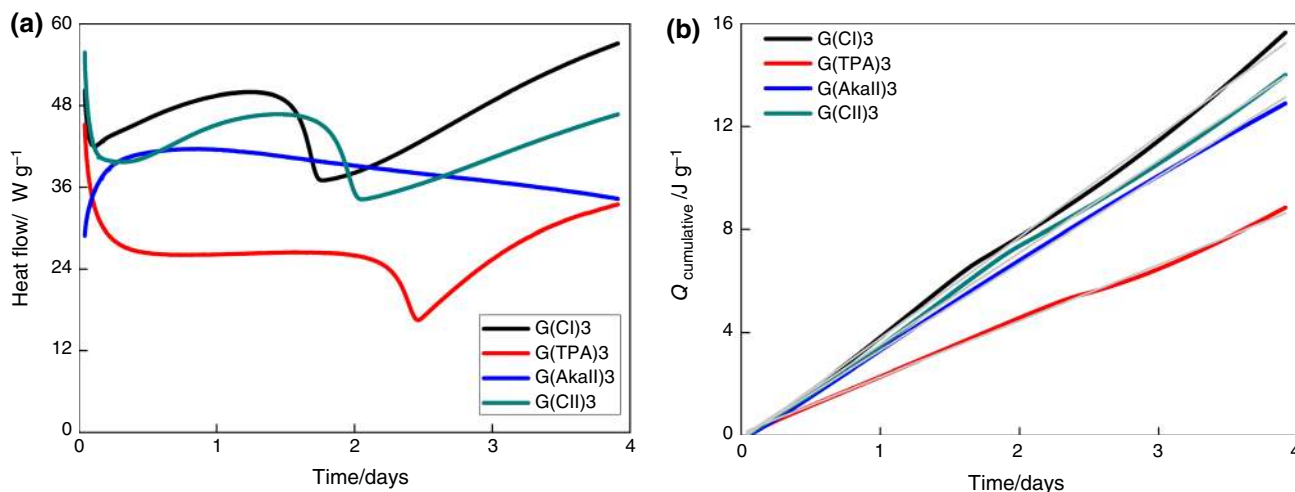


Fig. 2 **a** HFC curves, **b** cumulative heat versus time for granules containing nitrocellulose (13.3% N) and various stabilizers (centralite I, centralite II, triphenylamine, akardite II)

stabilizers. Thermal properties and chemical stability of granules containing TPA were better or similar in comparison to other stabilizers under study.

The effect of nitrogen content in nitrocellulose on the properties of nitrocellulose granules

The values of helium density, volume fraction of closed pores and the heat of combustion are presented in Table 4. In the group of granules containing centralite I, G(CI)3 was the one characterized by the lowest helium density (and the highest volume fraction of closed pores), while the other two granules G(CI)1 and G(CI)2 were characterized by a similar helium density and the volume fraction of closed pores. In the case of granules with TPA, the highest helium density (and the lowest volume fraction of closed pores) is characteristic to G(TPA)2 granulate. When comparing the granules with the same content of nitrogen in nitrocellulose, it can be observed that granules with TPA were characterized by lower values of helium density than the ones with CI (with the exception of NC 13.3% N). Lower values of helium density indicate that TPA has lower gelling properties than CI in the nitrocellulose matrix; thus, it is more

difficult to form granules with lower porosity. If the stabilizer is characterized by suitable gelling properties in the nitrocellulose matrix, then fibrous and porous structure of NC can be destroyed more easily.

The heat of combustion for granules with CI increases from 3079 to 3630 J g⁻¹ with the increasing nitrogen content in NC. The same dependence is observed for granules with TPA. As expected, the reduction in nitrogen content in nitrocellulose entails the decrease in the heat of combustion of granulate [48]. As mentioned before, the type of stabilizer does not entail a significant change of the heat of combustion when a nitrocellulose of the same nitrogen content is used.

DSC curves illustrated in Fig. 3 refer to the granules containing nitrocellulose with different nitrogen contents and stabilizers: centralite I or triphenylamine. Only one exothermic transition can be observed, similarly as this was the case of previous granules. The values of thermal properties (onset temperature, maximum temperature and enthalpy of decomposition) are presented in Table 4. The lowest maximum temperature of exothermic process is specific to the granules containing nitrocellulose with the highest nitrogen content (12.9 and 13.3% N). As expected, the maximum temperature of decomposition shifts toward higher temperatures with

Table 4 The properties of examined granules containing nitrocellulose with different nitrogen contents and various stabilizers (CI, TPA)

Samples	G(CI)2	G(CI)1		G(TPA)2		G(TPA)1	
$\rho_{He}/\text{g cm}^{-3}$	1.560 ± 0.006	1.552 ± 0.004		1.534 ± 0.004		1.476 ± 0.006	
$P_f/\%$	6.58 ± 0.36	7.07 ± 0.23		8.13 ± 0.26		11.6 ± 0.37	
$Q_c/\text{J g}^{-1}$	3399 ± 24	3079 ± 27		3366 ± 13		3067 ± 6	
$T_{\text{onset}}/^\circ\text{C}$	191.6	190.9	193.5	193.8	192.6	192	193
$T_{\text{max}}/^\circ\text{C}$	202.4	202.7	203.1	203.3	202	202.5	203.3
$\Delta H_d/\text{J g}^{-1}$	2106	2163	2069	2128	2175	2120	2254
$P_f/\mu\text{W g}^{-1}$	3.6	3.2		22.7		23.5	
$k_Q/\text{J g}^{-1} \text{ days}^{-1}$	4.04 ± 0.01	3.43 ± 0.01		1.86 ± 0.01		1.81 ± 0.01	

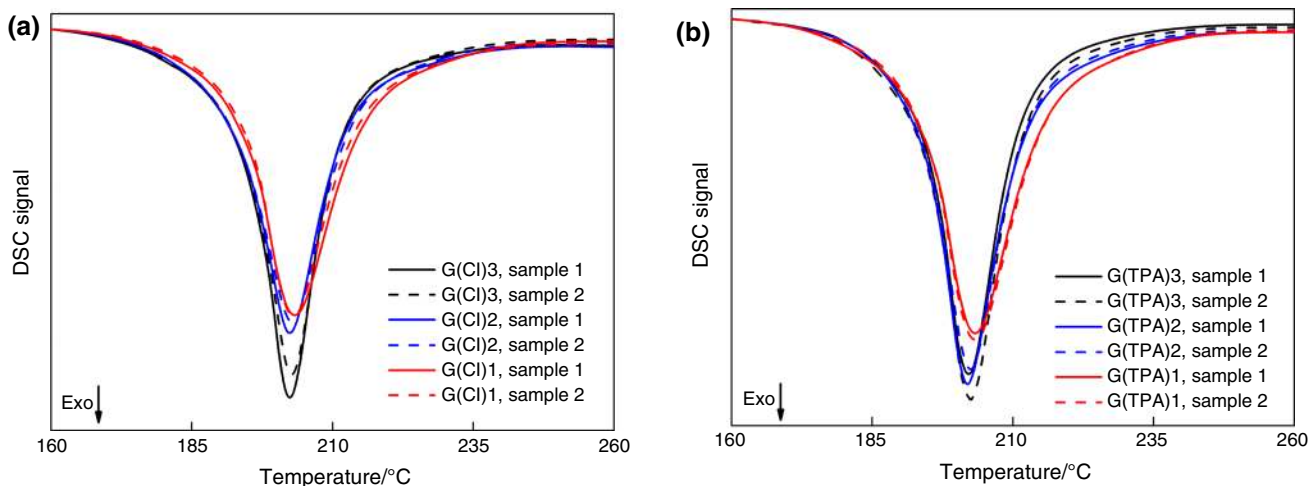


Fig. 3 DSC curves for granules containing nitrocellulose with different nitrogen contents and stabilizers: centralite I (a) or triphenylamine (b)

decreasing nitrogen content in NC for both type of granules containing CI and TPA as a stabilizer. Higher content of nitrogen in nitrocellulose makes the polymer less stable thermally, which translates into a decreased temperature of decomposition. The same effect of nitrogen content on thermal stability has been also reported, among others, by Pourmortazavi et al. or Chai et al. [2, 49]. The enthalpy average values of decomposition increase from 2099 to 2246 J g⁻¹ with increasing nitrogen content for granules containing CI, while for granules containing TPA, an inverse relationship was observed.

The dependence of heat flow versus function of time for granules containing nitrocellulose with different nitrogen contents and stabilizers: triphenylamine or centralite I, is shown in Fig. 4. All examined granules were characterized by a low heat flow signal as a function of time (below 60 μW g⁻¹), which means that they meet the requirements of STANAG 4582 standard. The shift of local minimum heat flow for granules containing CI and different shapes of curves for granules containing TPA can be related to the different kinetics of reaction these stabilizers with volatile products of NC decomposition. The higher the nitrogen content in nitrocellulose, the higher the concentration of nitrogen oxides, which affects the rate of formation of stabilizers derivatives.

The values for heat flow versus time $t_m=3.43/\text{days}$ (P_1) as well as constant heat generation rates are summarized in Table 4. The relationships of cumulative heat versus time and approximation by linear relations are shown in Supplementary Fig. S1 and S2. It has been observed that the heat generation rate decreases with decreasing nitrogen content in NC for granules with triphenylamine. For granules with CI, the lowest heat generation rate was obtained for granules with the lowest nitrogen content in NC, i.e., G(CI)1, while the other two granules were characterized by a similar value

of heat generation rate. All values of k_Q obtained for granules with TPA are lower than the heat generation rates for granules with CI. Lower values of both heat flow versus time and constant heat generation rate for TPA-containing granules indicate better nitrocellulose stabilizing properties than the granules containing a conventional stabilizer, such as CI.

Kinetic parameters of thermal decomposition for nitrocellulose granules

Kinetic parameters of thermal decomposition for selected granules were calculated to determine the effect of a stabilizer (samples G(CI)1 and G(TPA)1) and nitrogen content (samples G(TPA)1, G(TPA)2, G(TPA)3) in granules on kinetic parameters. The values of apparent energy activation and the logarithm of pre-exponential factor based on DSC and TG measurements are shown in Supplementary Tables S1–S4 for G(TPA)3, G(TPA)2, G(TPA)1 and G(CI)1, respectively.

The comparison of apparent activation energy versus the conversion degree (α) of granules containing nitrocellulose (12.2% N) and different stabilizers: TPA and CI, based on DSC measurements is presented in Fig. 5. The relationship between the apparent activation energy and conversion degree is associated with the overlap of many reactions occurring in the solid phase during decomposition process. Such relationships were observed for all tested granules. Changes in the apparent activation energy versus conversion degree are similar for G(CI)1 and G(TPA)1 granules. The apparent activation energy in the initial stage ($\alpha=0.05$) is equal to ${}_aE_a=171.4 \pm 3.6$ kJ mol⁻¹ for G(TPA)1 and ${}_aE_a=176.7 \pm 12.8$ kJ mol⁻¹ for G(CI)1. Initially, the apparent activation energy decreases to $\alpha=0.15$ and is equal to ${}_aE_a=161.6 \pm 1.7$ kJ mol⁻¹ for G(TPA)1, ${}_aE_a=167.2 \pm 4.9$ kJ mol⁻¹ for G(CI)1; then

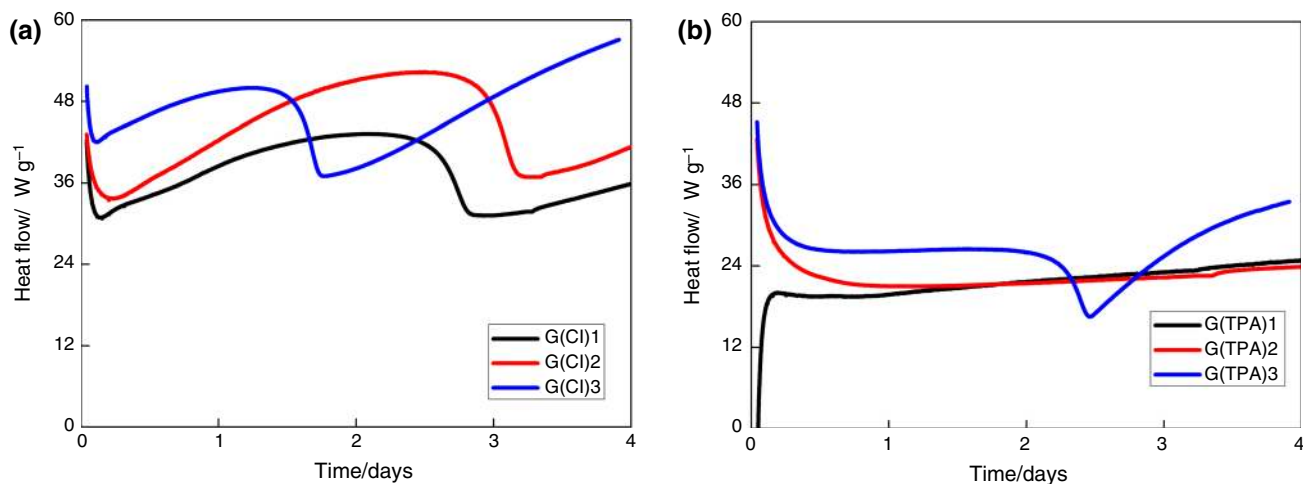


Fig. 4 HFC curves for granules containing nitrocellulose with different nitrogen contents and stabilizers: centralite I (a) or triphenylamine (b)

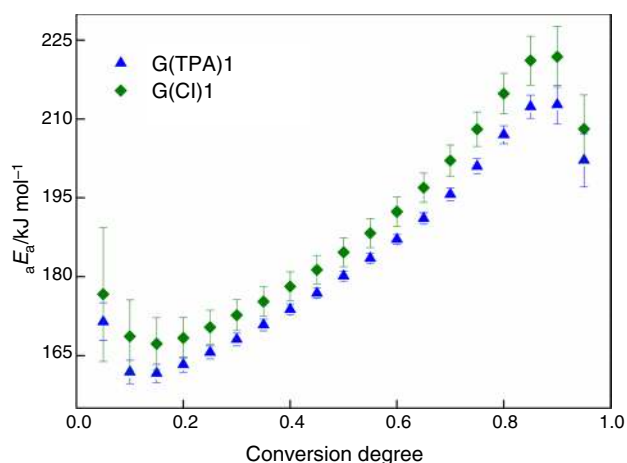


Fig. 5 Apparent activation energy (${}_aE_a$) versus conversion degree of granules containing nitrocellulose (12.2% N) and different stabilizers: TPA and CI, based on DSC measurements

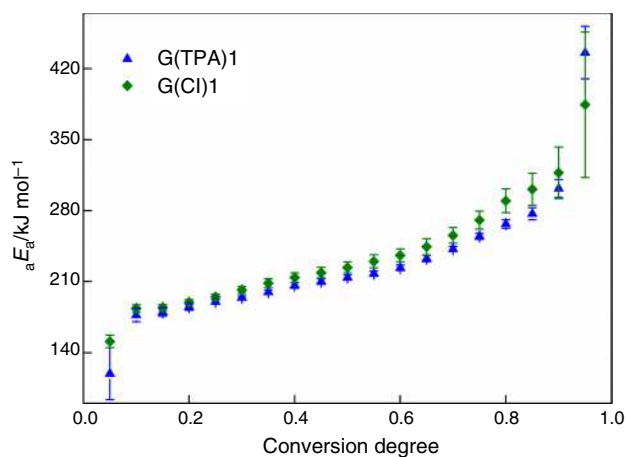


Fig. 6 Apparent activation energy (${}_aE_a$) versus the degree of conversion of granules containing nitrocellulose (12.2% N) and different stabilizers: TPA and CI, based on TG measurements

it gradually increases to the maximum for $\alpha = 0.90$ and is equal to ${}_aE_a = 212.8 \pm 3.7 \text{ kJ mol}^{-1}$ for G(TPA)1, ${}_aE_a = 221.8 \pm 5.8 \text{ kJ mol}^{-1}$ for G(CI)1. In the range of $\alpha = 0.05\text{--}0.95$, the apparent activation energy of G(CI)1 granule is higher than in case of G(TPA)1.

The relationship of apparent activation energy versus degree of conversion (α) of granules containing nitrocellulose (12.2% N) and different stabilizers: TPA and CI, based on TG measurements is presented in Fig. 6. Changes in the apparent activation energy versus conversion degree are similar for G(CI)1 and G(TPA)1 granules. The apparent activation energy in the initial stage ($\alpha = 0.05$) is equal to ${}_aE_a = 119.2 \pm 25.7 \text{ kJ mol}^{-1}$ for G(TPA)1 and ${}_aE_a = 151.2 \pm 6.2 \text{ kJ mol}^{-1}$ for G(CI)1. The apparent activation energy gradually increases to the maximum for $\alpha = 0.95$

and is equal to ${}_aE_a = 435.8 \pm 26.0 \text{ kJ mol}^{-1}$ for G(TPA)1, ${}_aE_a = 384.4 \pm 71.7 \text{ kJ mol}^{-1}$ for G(CI)1. In the range of $\alpha = 0.05\text{--}0.95$, the apparent activation energy of G(CI)1 granule is greater than for G(TPA)1; however, this difference between these values is smaller in TG analysis than in DSC measurements. No significant effect of stabilizer type on the change in apparent activation energy versus the degree of conversion was observed. The relationship of apparent activation energy versus the degree of conversion calculated on the basis of DSC and TG is characterized by lower values for low degree of conversion ($\alpha < 0.15$), and subsequently, the apparent activation energy increases with the degree of conversion. This is due to the fact that nitrocellulose decomposition products have an autocatalytic character and evolve slowly at the beginning of reaction. After autocatalytic products have been accumulated, the reaction rate increases rapidly. The same relationship for nitrocellulose was reported in the work of Chai et al. [49]. The different changes in the apparent activation energy versus conversion degree were observed for DSC and TG measurements. The apparent activation energy first decreases and then increases as the conversion degree increases for DSC measurements, while the apparent activation energy increases for TG measurements. Different processes occurred during DSC and TG measurements: decomposition reaction—DSC, and mass loss—TG. The rate of change of enthalpy is not directly proportional to the rate of mass loss [50]. The processes observed during thermal analysis depended on measurement conditions, the sample mass and the pan filling degree [40]. During the decomposition of high-energy materials, many parallel successive reactions can proceed. Determined kinetic parameters are the result of all the processes taking place during the decomposition of the sample [51].

The relationship of apparent activation energy versus the degree of conversion (α) of granules containing TPA and nitrocellulose with different nitrogen contents based on DSC measurements is presented in Fig. 7. Changes in the apparent activation energy versus the degree of conversion are similar for G(TPA)3, G(TPA)2, G(TPA)1 granules. The apparent activation energy in the initial stage ($\alpha = 0.05$) is equal to ${}_aE_a = 171.4 \pm 3.6 \text{ kJ mol}^{-1}$, $180.8 \pm 5.9 \text{ kJ mol}^{-1}$ and $188.5 \pm 4.0 \text{ kJ mol}^{-1}$ for G(TPA)1, G(TPA)2 and G(TPA)3, respectively. The minimum of the apparent activation energy is equal to ${}_aE_a = 161.6 \pm 1.7 \text{ kJ mol}^{-1}$, $170.8 \pm 1.5 \text{ kJ mol}^{-1}$ and $169.0 \pm 2.8 \text{ kJ mol}^{-1}$ for G(TPA)1, G(TPA)2 and G(TPA)3, respectively. Subsequently, the apparent activation energy gradually increases to the maximum for $\alpha = 0.90$ and is equal to ${}_aE_a = 212.8 \pm 3.7 \text{ kJ mol}^{-1}$, $235.2 \pm 7.7 \text{ kJ mol}^{-1}$ and $234.5 \pm 12.3 \text{ kJ mol}^{-1}$ for G(TPA)1, G(TPA)2 and G(TPA)3, respectively. In the range of $\alpha = 0.10\text{--}0.95$, the apparent activation energy of G(TPA)2 and G(TPA)3 granules is similar within the standard deviation tolerance and is higher than in the case of G(TPA)1.

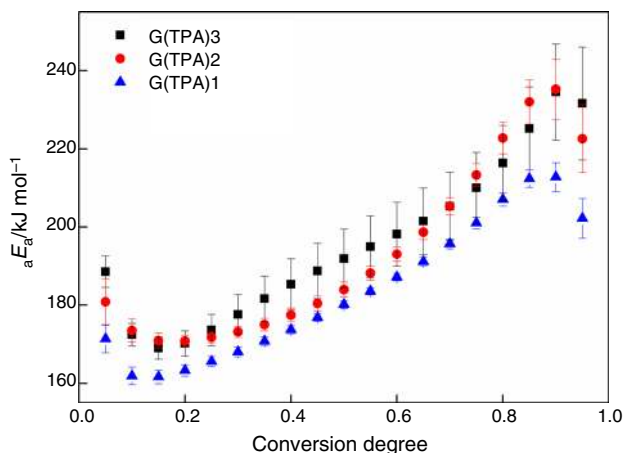


Fig. 7 The relationship of apparent activation energy (E_a) versus conversion degree of granules containing TPA and nitrocellulose with different nitrogen contents (12.2% N, 12.9% N, 13.3% N), based on DSC measurements

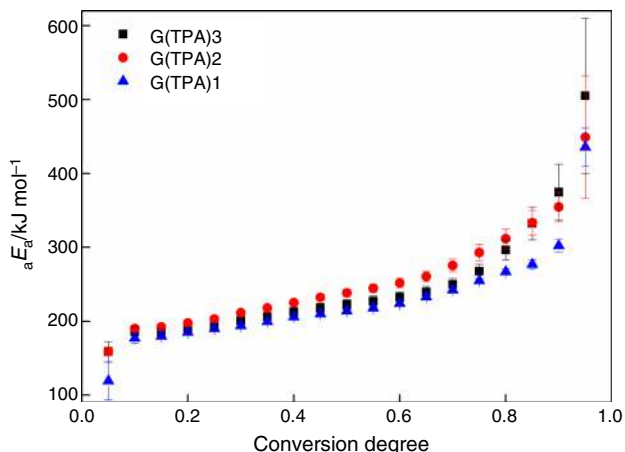


Fig. 8 The relationship of apparent activation energy (E_a) versus the degree of conversion of granules containing TPA and nitrocellulose with different nitrogen contents (12.2% N, 12.9% N, 13.3% N), based on TG measurements

The relationship of apparent activation energy versus the degree of conversion (α) of granules containing TPA and nitrocellulose with different nitrogen contents based on TG measurements is presented in Fig. 8. Changes in the apparent activation energy versus degree of conversion are similar for G(TPA)3, G(TPA)2, G(TPA)1 granules. The apparent activation energy in the initial stage ($\alpha = 0.05$) is equal to $E_a = 119.2 \pm 25.7 \text{ kJ mol}^{-1}$, $159.2 \pm 5.8 \text{ kJ mol}^{-1}$ and $158.6 \pm 13.7 \text{ kJ mol}^{-1}$ for G(TPA)1, G(TPA)2 and G(TPA)3, respectively. The apparent activation energy gradually increases to the maximum for $\alpha = 0.95$ and is equal to $E_a = 435.8 \pm 26.0 \text{ kJ mol}^{-1}$, $449.2 \pm 83.0 \text{ kJ mol}^{-1}$, $504.9 \pm 104.9 \text{ kJ mol}^{-1}$ for G(TPA)1, G(TPA)2 and

G(TPA)3, respectively. In the range of $\alpha = 0.05\text{--}0.90$, the apparent activation energy of G(TPA)2 and G(TPA)3 granules is similar within the standard deviation tolerance and is higher than in the case of G(TPA)1.

The change in nitrogen content in nitrocellulose does not entail modification in the nature of changes in the apparent energy of activation versus degree of conversion. It was observed that, in a significant scope of degrees of conversion, the NC-containing granules of the lowest nitrogen content are characterized by the lowest apparent energy of activation energy. The other two granules, G(TPA)2 and G(TPA)3 with higher nitrogen content, are characterized by similar values of apparent activation energy within the error margin. Chai et al. [49] observed that in the initial stage of the reaction, the activation energy increases with the decrease in nitrocellulose nitrogen content, while for the higher degrees of conversion, an inverse relationship was observed. The introduction of stabilizer to nitrocellulose entails a change in the relationship of apparent activation energy versus the nitrogen content at the initial stage of reaction.

The study of adjusting experimental data to various kinetic models was performed. Based on the calculations, the obtained kinetic model of all granules is n th order with autocatalysis (CnB)—correlation coefficients, are above 0.98 for all examined granules. This kinetic model can be demonstrated by a general equation [52]:

$$d\alpha/dt = A \cdot \exp(-E/RT) \cdot (1 - \alpha)^n \cdot (1 + K_{cat} \cdot \alpha) \quad (3)$$

where n is reaction order, K_{cat} the balance constant for autocatalysis reaction.

The calculated values of activation energy (E), logarithm of pre-exponential factor ($\log A$), reaction order (n) and the logarithm of the balance constant for autocatalysis reaction ($\log K_{cat}$) for kinetic model CnB of examined granules are presented in Tables 5 and 6 for DSC and TG measurements, correspondingly. The reaction order for all examined granules is contained in the range from 2.3 to 2.5, based on DSC measurements, and 2.9–3.3, based on TG measurements. The activation energy (E) increases with increasing of nitrogen content in nitrocellulose granules from 189.5 to 218.7 kJ mol^{-1} for DSC measurements. The granules containing nitrocellulose with 12.9% N are characterized by the highest value of activation energy (238.6 kJ mol^{-1}) for TG measurements. The granules containing centralite I as stabilizer are characterized by a higher value of the activation energy than the granules with TPA (with the same nitrogen content in nitrocellulose) in both DSC and TG measurements.

It should be noted, however, that resultant activation energy values for stabilizer-containing granules are higher than the activation energy for pure

Table 5 Calculated values of activation energy (E), logarithm of pre-exponential factor ($\log A$), reaction order (n) and the logarithm of the balance constant for autocatalysis reaction ($\log K_{\text{cat}}$) for kinetic model CnB based on DSC measurements of G(TPA)3, G(TPA)2, G(TPA)1, G(CI)1 granules

Samples	G(TPA)3	G(TPA)2	G(TPA)1	G(CI)1
$\log(A/s^{-1})$	21.15 ± 0.01	19.27 ± 0.04	17.85 ± 0.01	18.05 ± 0.01
$E/kJ\ mol^{-1}$	218.7 ± 0.1	201.7 ± 0.4	189.5 ± 0.1	190.8 ± 0.1
n	2.40 ± 0.03	2.34 ± 0.01	2.49 ± 0.01	2.44 ± 0.01
$\log K_{\text{cat}}$	1.53 ± 0.02	1.47 ± 0.01	1.49 ± 0.01	1.42 ± 0.01
Correlation coefficient	0.9800	0.9974	0.9977	0.9976

Table 6 Calculated values of activation energy (E), logarithm of pre-exponential factor ($\log A$), reaction order (n) and the logarithm of the balance constant for autocatalysis reaction ($\log K_{\text{cat}}$) for kinetic model CnB based on TG measurements of G(TPA)3, G(TPA)2, G(TPA)1, G(CI)1 granules

Samples	G(TPA)3	G(TPA)2	G(TPA)1	G(CI)1
$\log(A/s^{-1})$	23.26 ± 0.03	23.85 ± 0.02	21.03 ± 0.06	22.15 ± 0.03
$E/kJ\ mol^{-1}$	232.4 ± 0.5	238.6 ± 0.4	212.7 ± 0.6	222.9 ± 0.4
n	2.92 ± 0.02	3.23 ± 0.02	3.12 ± 0.01	3.27 ± 0.02
$\log K_{\text{cat}}$	0.94 ± 0.05	1.09 ± 0.05	0.79 ± 0.02	0.84 ± 0.04
Correlation coefficient	0.9950	0.9967	0.9980	0.9974

Table 7 Collation of activation energy (E_a) of thermal decomposition of nitrocellulosis obtained with various methods

Method	Nitrogen content in NC	Model	$E_a/kJ\ mol^{-1}$	Ref.
Microcalorimeter	11.98	Isothermal method by Vyazovkin	89.03	[49]
	12.87		72.37	
Isothermal decomposition	12.76	Arrhenius equation	146.3	[28]
	TG	13.9	ASTM method	156.8
Ozawa method			154.0	
TG	11.96	Kissinger–Akahira–Sunose method	148.6	[53]
		Friedman method	154.3	

nitrocellulose—exemplary literature data are collated in Table 7.

Conclusions

The examinations of physicochemical and thermal properties allowed to expand the knowledge on the effect of stabilizers and nitrogen content on the parameters of nitrocellulose granules. The helium density of resultant granules ranged from 1.48 to 1.56 g cm⁻³. It was observed that the helium density of granules depends on the degree of nitrocellulose gelling by the stabilizer. The heat of combustion does not rely on the type of stabilizer used, whereas the increase in nitrogen content in nitrocellulose increases the heat of combustion (from 3079 to 3630 J g⁻¹). In DSC analysis, a rapid/uncontrolled thermal decomposition was observed for granules containing the

highest nitrogen content, i.e., 13.3% N. A thermal stability of granules (determined on the basis of DSC and HFC analysis) increases with the decrease in nitrogen content in nitrocellulose. All resulting granules meet the requirements laid down in STANAG 4582, which means that they are chemical stable when stored at 25 °C for 10 years.

The change in nitrogen content in nitrocellulose does not entail modification in relationship of apparent activation energy versus degree of conversion. It was observed that in a significant scope of degrees of conversion, G(TPA)1 granule is characterized by the lowest apparent energy of activation. The introduction of stabilizer to nitrocellulose entails a different effects of nitrogen content on the apparent energy of activation, i.e., apparent activation energy increases with increased nitrogen content.

A chemical reaction model was adapted— n th order with autocatalysis (CnB) for all studied granules, based on both DSC and TG measurements. Reaction order ranged

from 2.3 to 3.3, while the activation energy—from 190 to 239 kJ mol⁻¹ depending on the content of nitrogen and measurement method (DSC or TG). According to literature sources, resultant values of activation energy for stabilizer-containing granules are higher than the corresponding values for pure nitrocellulose.

Open Access This article is licensed under a Creative Commons Attribution 4.0 International License, which permits use, sharing, adaptation, distribution and reproduction in any medium or format, as long as you give appropriate credit to the original author(s) and the source, provide a link to the Creative Commons licence, and indicate if changes were made. The images or other third party material in this article are included in the article's Creative Commons licence, unless indicated otherwise in a credit line to the material. If material is not included in the article's Creative Commons licence and your intended use is not permitted by statutory regulation or exceeds the permitted use, you will need to obtain permission directly from the copyright holder. To view a copy of this licence, visit <http://creativecommons.org/licenses/by/4.0/>.

References

- de la Ossa MAF, Torre M, García-Ruiz C. Nitrocellulose in propellants: characteristics and thermal properties. In: Wythers MC, editor. *Advances in materials science research*, vol. 7. Hauppauge: Nova Science Publishers; 2012. p. 201–20.
- Pourmortazavi SM, Hosseini SG, Rahimi-Nasrabadi M, Hajmirsadeghi SS, Momenian H. Effect of nitrate content on thermal decomposition of nitrocellulose. *J Hazard Mater*. 2009;162:1141–4.
- Fryš O, Bajerová P, Eisner A, Skládal J, Ventura K. Utilization of new non-toxic substances as stabilizers for nitrocellulose-based propellants. *Propellants Explos Pyrotech*. 2011;36:347–55.
- Wilker S, Heeb G, Vogelsanger B, Petržílek J, Skládal J. Triphenylamine—a ‘New’ stabilizer for nitrocellulose based propellants—part I: chemical stability studies. *Propellants Explos Pyrotech*. 2007;32:135–48.
- Katoh K, Yoshino S, Kubota S, Wada Y, Ogata Y, Nakahama M, Kawaguchi S, Arai M. The effects of conventional stabilizers and phenol compounds used as antioxidants on the stabilization of nitrocellulose. *Propellants Explos Pyrotech*. 2007;32:314–21.
- Trache D, Tarchoun AF. Stabilizers for nitrate ester-based energetic materials and their mechanism of action: a state-of-the-art review. *J Mater Sci*. 2018;53:100–23.
- Gańczyk K, Książczak A. Phase transitions in binary system: nitrocellulose + stabilizer. *New trends in research of energetic materials*. In: *Proceedings of the seminar, 17th, Pardubice, Czech Republic, 2014*; pp. 209–219.
- Błądek J, Cudziło S, Pietrzyk S, Wilker S. A novel method for testing propellant stabilizers. *Central Eur J Energ Mater*. 2010;7:281–7.
- Curtis NJ, Kempson RM, Turner AR, White A. *Alternative stabilisers: reactivity and analysis*. Oceania: DSTO External Publications; 1990.
- Dejeaifve A, Dobson R. Tocopherol stabilisers for nitrocellulose-based propellants. US20180029952A1, 2018.
- Dejeaifve A, Berton V, Dobson R. Stabilized nitrocellulose-based propellant composition. EP3052458B1, 2016.
- Dejeaifve A, Dobson R. Ionone stabilisers for nitrocellulose-based propellants. US20180029951A1, 2018.
- Dejeaifve A, Fantin A, Monsieur L, Dobson R. Making progress towards «Green» propellants. *Propellants Explos Pyrotech*. 2018;43:831–7.
- Fredrich O, Tibbitts GC, Kerone EBW. *Manufacture of smokeless powders*. US2027114A, 1936.
- Wu Y, Luo Y, Ge Z. Properties and application of a novel type of glycidyl azide polymer (GAP)-modified nitrocellulose powders. *Propellants Explos Pyrotech*. 2015;40:67–73.
- Andrew EA, Halverson HJ. *Manufacture of globular powder*. US3679782A, 1972.
- Thomas KA. *Continuous production of low density base grain with a salt-free liquor*. US4694753A, 1987.
- Wu Y, Yi Z, Luo Y, Ge Z, Du F, Chen S, Sun J. Fabrication and properties of glycidyl azide polymer-modified nitrocellulose spherical powders. *J Therm Anal Calorim*. 2017;129:1555–62.
- Stoetzer E, Wassmuth H, Abraham A. *Process for the manufacture of low density nitrocellulose granules*. US3824108A, 1974.
- Earnest SC. *Smokeless powder process*. US2375175A, 1945.
- Holmes RS, Baldrige BC, O’neill JJJ, Earnest SC. *Propellant*. US2771351A, 1956.
- Dehn FB. *Smokeless Propellant Powder and the Process of Making the Same*. GB473057A, 1937.
- Староверов АА, Гагина Р, Хацринов АИ, Староверова ЕИ, Абдулкаюмова СМ, Михайлов ЮМ, Имамиева АР, Ложкина ЛЕ. *Ball powder for 5,6 mm sports rifle cartridge of ring ignition*. RU2503648C2, 2012.
- Gańczyk-Specjalska K, Gołofit T, Jamroga K. The application of nitrocellulose and ammonium perchlorate granules for solid rocket propellants formed by loading method. *New trends in research of energetic materials*. In: *Proceedings of the Seminar, 21st, Pardubice, Czech Republic, 2018*, pp. 554–563.
- Abramov VG, Vaganova NI. Effect of a side reaction with small heat liberation on the critical thermal-explosion condition of the main self-catalyzed reaction. *Fiz Goreniya Vzryva*. 1978;14:135–41.
- Semenov NN. *Chemical kinetics and chain reactions*. London: Oxford University Press; 1935.
- Luo Q, Ren T, Shen H, Zhang J, Liang D. The thermal properties of nitrocellulose: from thermal decomposition to thermal explosion. *Combust Sci Technol*. 2018;190:579–90.
- Luo L, Jin B, Xiao Y, Zhang Q, Chai Z, Huang Q, Chu S, Peng R. Study on the isothermal decomposition kinetics and mechanism of nitrocellulose. *Polymer Testing*. 2019;75:337–43.
- Shehata A, Hassan M. Poly N-(4-chlorophenyl), poly N-(4-methylphenyl) acrylamides and the copolymer of their monomers as stabilizers for nitrocellulose. *Polym Degrad Stab*. 2002;77:355–70.
- Moniruzzaman M, Bellerby JM, Bohn MA. Activation energies for the decomposition of nitrate ester groups at the anhydroglucopyranose ring positions C2, C3 and C6 of nitrocellulose using the nitration of a dye as probe. *Polym Degrad Stab*. 2014;102:49–58.
- Chelouche S, Trache D, Tarchoun AF, Abdelaziz A, Khimeche K, Mezroua A. Organic eutectic mixture as efficient stabilizer for nitrocellulose: kinetic modeling and stability assessment. *Thermochim Acta*. 2019;673:78–91.
- Hassan M. Effect of malonyl malonanilide dimers on the thermal stability of nitrocellulose. *J Hazard Mater*. 2001;88:33–49.
- Pourmortazavi SM, Kohsari I, Zandavar H, Foroutan Koudehi M, Mirsadeghi S. Electrospinning and thermal characterization of nitrocellulose nanofibers containing a composite of diamino-furazan, aluminum nano-powder and iron oxide nanoparticles. *Cellulose*. 2019;26:4405–15.
- Chen L, Bromberg L, Hatton TA, Rutledge GC. Electrospun cellulose acetate fibers containing chlorhexidine as a bactericide. *Polymer*. 2008;49:1266–75.

35. Pourmortazavi SM, Farhadi K, Mirzajani V, Mirzajani S, Kohsari I. Study on the catalytic effect of diaminoglyoxime on thermal behaviors, non-isothermal reaction kinetics and burning rate of homogeneous double-base propellant. *J Therm Anal Calorim.* 2016;125:121–8.
36. Mirzajani V, Farhadi K, Pourmortazavi SM. Catalytic effect of lead oxide nano- and microparticles on thermal decomposition kinetics of energetic compositions containing TEGDN/NC/DAG. *J Therm Anal Calorim.* 2018;131:937–48.
37. Sovizi MR, Hajimirsadeghi SS, Naderizadeh B. Effect of particle size on thermal decomposition of nitrocellulose. *J Hazard Mater.* 2009;168:1134–9.
38. Luo L, Jin B, Xiao Y, Zhang Q, Chai Z, Huang Q, Chu S, Peng R. Study on the isothermal decomposition kinetics and mechanism of nitrocellulose. *Polym Test.* 2019;75:337–43.
39. Gołofit T. Thermal behaviour and safety of 1,3,7,9-tetranitro-*ibenzo-1,3a,4,6a-tetraazapentalen (z-TACOT)*. *Thermochim Acta.* 2018;667:59–64.
40. Gańczyk K, Zygmunt A, Gołofit T. Thermal properties of TEX decomposition or sublimation. *J Therm Anal Calorim.* 2016;125:967–75.
41. Vyazovkin S, Chrissafis K, Di Lorenzo ML, Koga N, Pijolat M, Roduit B, Sbirrazzuoli N, Suñol JJ. ICTAC Kinetics Committee recommendations for collecting experimental thermal analysis data for kinetic computations. *Thermochim Acta.* 2014;590:1–23.
42. Maj J. Explosives, nitrocellulose based propellants, stability test procedure and requirements using heat flow calorimetry. STANAG 4582. (Edition 1). 2007;A/1–C/1.
43. Tomaszewski W, Cieślak K, Zygmunt A. Influence of processing solvents on decomposition of nitrocellulose in smokeless powders studied by heat flow calorimetry. *Polym Degrad Stab.* 2015;111:169–75.
44. Vyazovkin S, Burnham AK, Criado JM, Pérez-Maqueda LA, Popescu C, Sbirrazzuoli N. ICTAC Kinetics Committee recommendations for performing kinetic computations on thermal analysis data. *Thermochim Acta.* 2011;520:1–19.
45. Yao F, Wu Q, Lei Y, Guo W, Xu Y. Thermal decomposition kinetics of natural fibers: activation energy with dynamic thermogravimetric analysis. *Polym Degrad Stab.* 2008;93:90–8.
46. Rosu L, Mustata F, Varganici C, Rosu D, Rusu T, Rosca I. Thermal behaviour and fungi resistance of composites based on wood and natural and synthetic epoxy resins cured with maleopimaric acid. *Polym Degrad Stab.* 2019;160:148–61.
47. Meyer R, Köhler J, Homburg A. *Explosives*. 6th ed. New York: Wiley; 2007.
48. Davenas A. *Double-base propellants. Solid rocket propulsion technology*. 1st ed. Oxford: Pergamon Press; 1993. p. 369–414.
49. Chai H, Duan Q, Jiang L, Gong L, Chen H, Sun J. Theoretical and experimental study on the effect of nitrogen content on the thermal characteristics of nitrocellulose under low heating rates. *Cellulose.* 2019;26:763–76.
50. Agrawal RK. Analysis of non-isothermal reaction kinetics. Part 2. Complex reactions. *Thermochim Acta.* 1992;203:111–25.
51. Gołofit T, Zysk K. Thermal decomposition properties and compatibility of CL-20 with binders HTPB, PBAN, GAP and polyN-IMMO. *J Therm Anal Calorim.* 2015;119:1931–9.
52. Wang H, Zhang H, Hu R, Yao E, Guo P. Estimation of the critical rate of temperature rise for thermal explosion of nitrocellulose using non-isothermal DSC. *J Therm Anal Calorim.* 2014;115:1099–110.
53. Wei R, He Y, Zhang Z, He J, Yuen R, Wang J. Effect of different humectants on the thermal stability and fire hazard of nitrocellulose. *J Therm Anal Calorim.* 2018;133:1291–307.

Publisher's Note Springer Nature remains neutral with regard to jurisdictional claims in published maps and institutional affiliations.